

M. ZIĘTAŁA\*<sup>#</sup>, T. DUREJKO\*, M. ŁAZIŃSKA\*

**WIRE ELECTRICAL DISCHARGE MACHINING OF FEAL INTERMETALLIC SINTERS WITHOUT AND WITH ADDITION OF NANO- $\text{Al}_2\text{O}_3$  OXIDE CERAMIC**

**OBRÓBKA ELEKTROEROZYJNA SPIEKÓW NA OSNOWIE FAZY MIĘDZYMETALICZNEJ FEAL BEZ I Z DODATKIEM NANOCERAMIKI  $\text{Al}_2\text{O}_3$**

The influence of the parameters of wire electrical discharge machining (WEDM) on the surface layer of FeAl based sinters with and without  $\text{Al}_2\text{O}_3$  nanoceramic addition has been studied in this paper. The properties of the sinters surface layer were controlled by WEDM parameters, including time of interval ( $t_p$ ) and amplitude of current ( $I_A$ ). The WEDM roughing and finishing treatments were carried out for selected technological parameters of process. The surface texture (ST) of the sinters after WEDM was analyzed by profilometer method. Theoretical parameters describing abrasive wear resistance of investigated sinters were estimated on the basis on the load capacity curve.

On the basis on obtained results it can be stated that there is possibility of shaping geometry of nano- $\text{Al}_2\text{O}_3$  doped and undoped FeAl sinters by WEDM. Reduction of the time of interval ( $t_p$ ) and increase of current amplitude ( $I_A$ ) during WEDM deteriorate surface properties. Addition of nano- $\text{Al}_2\text{O}_3$  improve the quality of the obtained surface. Applied parameters of WEDM improve theoretical abrasive wear resistance and lubricant maintenance of the nanoceramic doped material in comparison with undoped sinter.

*Keywords:* surface texture (ST), abrasive wear resistance, wire electrical discharge machining (WEDM), FeAl intermetallic, nano- $\text{Al}_2\text{O}_3$  addition

W niniejszej pracy analizowano wpływ parametrów cięcia elektroerozyjnego (ang. WEDM – wire electrical discharge machining) na warstwę wierzchnią spieków na osnowie fazy międzymetalicznej FeAl bez i z dodatkiem nanoceramiki  $\text{Al}_2\text{O}_3$ . Poprzez zmianę parametrów obróbki elektroerozyjnej, tj. czas przerwy ( $t_p$ ) i natężenie prądu ( $I_A$ ), sterowano właściwościami warstwy wierzchniej obrabianych spieków. Dla wybranych parametrów technologicznych procesu przeprowadzono obróbkę zgrubną i wykańczającą. Strukturę geometryczną powierzchni (SGP) spieków po obróbce elektroerozyjnej analizowano za pomocą metody profilometrycznej. Parametry charakteryzujące teoretyczną odporność na zużycie ściernie zostały oszacowane na podstawie krzywych nośności Abbotta-Firestone’a.

Na podstawie uzyskanych wyników stwierdzono, że istnieje możliwość kształtowania geometrii spieków FeAl bez i z dodatkiem nanoceramiki  $\text{Al}_2\text{O}_3$  za pomocą obróbki elektroerozyjnej WEDM. Wraz ze skróceniem czasu przerwy i wzrostem natężenia prądu podczas obróbki wzrasta chropowatość obrabianych powierzchni, natomiast dodatek nanoceramiki poprawia jakość otrzymanych powierzchni. Zastosowane parametry obróbki WEDM poprawiły teoretyczną odporność na zużycie ściernie i zdolność do przechowywania środka smarnego powierzchni spieków domieszkowanych nanoceramiką, w porównaniu do materiału niedomieszkowanego.

## 1. Introduction

One of the alternative method of shaping the geometry of machines components is the electrical discharge machining (EDM), currently used in the aerospace and automotive industries. This technology allows obtaining elements with complex geometry and with precisely shaped surface texture (ST) due to proper selection of such processing parameters as:

amplitude, time of impulse or interval time [1-3]. The process of electrical discharge machining allows controlling of geometry and surface texture of the surface layer, determined by its application features. EDM can be applied to elements made of any electrically conductive material, regardless of their strength and hardness. Kind of processed material has only influence on the selection of technological parameters, which in turn affects the efficiency and intensity of erosion wear. The erosion-based

\* DEPARTMENT OF ADVANCED MATERIALS AND TECHNOLOGY, MILITARY UNIVERSITY OF TECHNOLOGY, 2 KALISKIEGO STR., 00-908 WARSAW, POLAND

# Corresponding author: mzietal@wat.edu.pl

shaping technique of machine components is also used for processing of metal matrix composites [3-6]. A main obstacle in introducing traditional machining methods to processing of these materials is reinforcement phase in the form of particles, fibers or precipitates [5]

Results of several years of research conducted in Department of Advanced Materials and Technologies of MUT have revealed that the use of electrical discharge machining with numerically controlled wire cutter (WEDM) allows shaping of such materials as FeAl intermetallic alloys [7]. These alloys belong to group of materials which can be applied at high temperature, close to their melting points with simultaneously meeting increasing requirements stated by designers and engineers – high wear resistance and very good resistance to high-temperature corrosion [8-10]. However a high brittleness and a low creep resistance of Fe-Al based alloys effectively limit area of their applications. These materials can be produced by a conventional melting and casting, but finally obtained coarse-grained structure required further multivariant thermo-mechanical treatment [11-14]. Nowadays, Fe-Al intermetallics are usually used as a protective coatings deposited by a detonation gas spraying [15-24] and a laser cladding [25-28]) or as reactive, exothermic mixtures (consisted of Fe and Al elemental powder) for joining other materials (e.g. in the form of thin foils) [29]. A chance for manufacturing a bulk FeAl intermetallics parts could be an apply techniques based on metallurgy of technically pure iron and aluminum powders [30-32] or an implementation of a laser deposition method to produce a FeAl/metal gradient structure [33].

It was also previously shown, that doping with alumina particles has beneficial effect on high temperature behaviour of these alloys [34-36]. Refinement and strengthening of structure by alumina ceramics particles allow controlling properties of FeAl alloys, especially in the field of their high temperature applications (e.g. increase of creep resistance). Due to presence of oxide ceramic (with high abrasive wear resistance), abnormal increase of yield strength with rising temperature and lower cohesive strength in the grain boundaries than for as cast materials, these alloys are classified as hard to machine materials [1,37,38]. These features effectively reduce or eliminate possibility of using conventional machining methods (such as turning, milling, etc.) to FeAl intermetallic sinters. The chance for commercial forming of semi-finished products made of these alloys is electrical discharge machining. The application of electrical discharge machining with a numerically controlled wire cutter (WEDM) allows obtaining elements with complex geometry (2,5D) and with a precisely shaped surface texture (ST) of finished product. Recently, WEDM is used to machine a wide variety of miniature and micro-parts from metals [39-40], sintered materials, alloys [41], cemented carbides and ceramics [42-43]. Therefore, the treatment of this type should enable the development of both the geometry and the surface texture of FeAl intermetallic sinters with and without the addition of nano- $\text{Al}_2\text{O}_3$  ceramics.

In present work, the result of the parameters selection for electrical discharge machining roughing and finishing of FeAl sinters doped and non-doped nano- $\text{Al}_2\text{O}_3$  have been presented.

Selection of WEDM treatment parameters allows controlling surface texture features and theoretical assessment of the abrasive wear.

## 2. Investigated material

The investigated material was obtained in the sintering process at low pressure ( $10^{-2}$  mBar) at  $1050^\circ\text{C}$  and under a constant load of 40 MPa. The feedstock material was a mixture of technically pure aluminum and Fe-nano- $\text{Al}_2\text{O}_3$  composite powder (2% vol. addition of nano- $\text{Al}_2\text{O}_3$  ceramic, obtained by low-energetic milling in a Fritsch ball-mill with a velocity of 200 rpm and milling time of 20 minutes [44] or mixture of technically pure aluminum and iron. Both variants have been prepared in 60 to 40 at.% iron to aluminum ratio. After pre-sintering process sinters were homogenized by annealing process at  $1200^\circ\text{C}$  for 1 hour in an argon atmosphere.

Quantitative metallographic investigations were done by using Philips XL30/LaB6 scanning electron microscope equipped in backscattered electrons detector (BSE) and energy dispersive spectrometry (EDS) dedicated to chemical composition analysis. Sintered FeAl intermetallic alloys, without and with the addition of nanoceramic, had a single-phase and fine-grained structure. Structural investigations of the sinters revealed chemical homogeneity of their matrix (FeAl phase) and presence of micro oxide particles ( $\text{Al}_2\text{O}_3$ ) among the FeAl grain boundaries (Fig. 1a). Sintors with addition of nano- $\text{Al}_2\text{O}_3$  additionally possessed nanometric  $\text{Al}_2\text{O}_3$  particles distributed inside grain areas (Fig. 1b). The results of the analysis of chemical composition, density, porosity and the average grain size of the samples are listed in Table 1 [44].

TABLE 1

Summary of chemical composition, density and porosity of FeAl sinters with and without addition of  $\text{Al}_2\text{O}_3$  nanoceramic [44]

Material	FeAl		FeAl+nano- $\text{Al}_2\text{O}_3$	
Chemical composition				
Element	wt.%	at. %	wt. %	at. %
O	2,32	6,11	4,28	10,81
Al	24,91	38,93	25,74	38,55
Fe	72,78	54,96	69,98	50,64
Total	100	100	100	100
Theoretical density [ $\text{g}/\text{cm}^3$ ]	6,06		5,93	
Measured density [ $\text{g}/\text{cm}^3$ ]	5,81		5,56	
Porosity [%]	4,2		6,2	
Equivalent circle diameter (ECD) grain size [ $\mu\text{m}$ ]	$3,9 \pm 1,69$		$3,8 \pm 1,42$	

## 3. Experimental details

After a full cycle of heat treatment, the sinters were machined with an electric discharge device with a numerically controlled wire cutter BP-97d. During cutting (perpendicular to pressing direction) a brass wire of 0.25 mm in diameter and

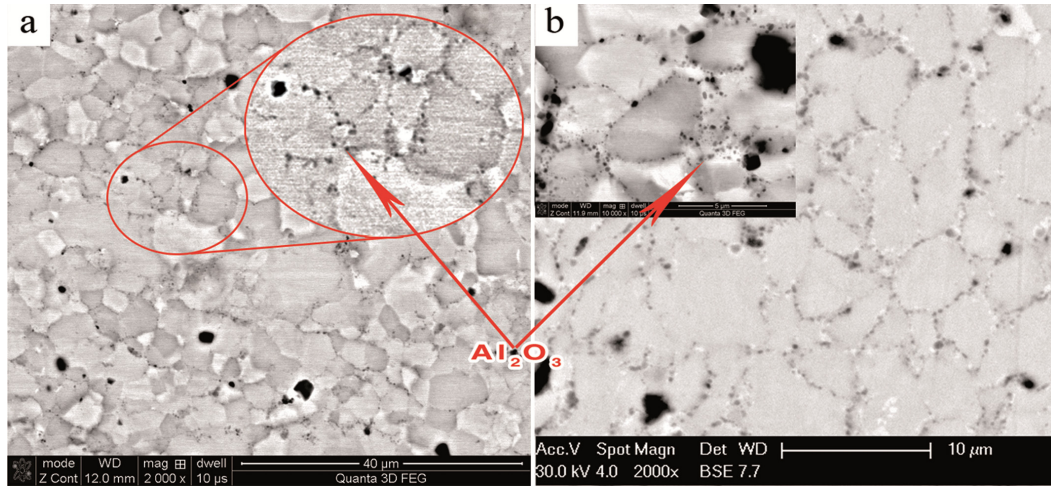


Fig. 1. Microstructure of FeAl sinter: a) without the addition of nanoceramic Al<sub>2</sub>O<sub>3</sub>, b) with 2% vol. of Al<sub>2</sub>O<sub>3</sub> addition

tensile strength of 500 MPa was used. The operating conditions were controlled by the duration of the interval between impulses  $t_p$  and current amplitude  $I_A$ . For selected couples of processing parameters (time interval – current amplitude) roughing treatment was done, during which the FeAl samples were cut. Moreover, then finishing treatment consisting of four sparking passes was done (without surface wire penetration).

Preliminary observations of the sinters surface after WEDM revealed formation of scale on the samples (Fig. 2a). Numerous cracks and discontinuities occur on scale surface and in the place where „clean“ sinter surface is visible (Fig. 2a). To avoid the

formation of oxidized layer after WEDM process the head feed was increased, what results in reduction of the time in which the material was subjected to high temperature and negative influence of deionized water and atmospheric oxygen. Intensity of the working gap flushing was also increased. Additionally, sample was purified in an ultrasonic bath directly after cutting. As result “clear”, scaleless sample surface was obtained (Fig. 2b).

After the modification of multivariate WEDM process of FeAl sinters with and without nano-Al<sub>2</sub>O<sub>3</sub> was carried out, according to the parameters listed in Table 2. The impulse duration, feed, wire feed and force of wire tension were adopted as constant

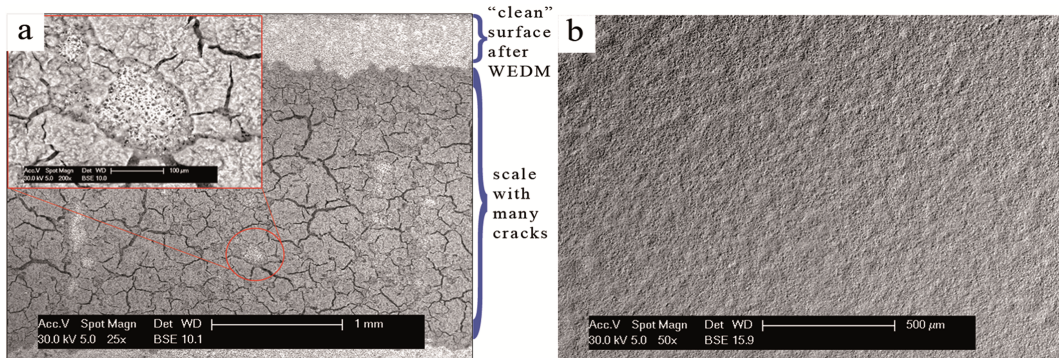


Fig. 2. Sample surface after WEDM process: a) with a visible layer of scale, b) after the initial modification of WEDM parameters and cleaning in an ultrasonic cleaner

TABLE 2

Parameters of wire electrical discharge machining (WEDM) of FeAl and FeAl + nano-Al<sub>2</sub>O<sub>3</sub> sinters

FeAl			
Treatment option	Type of treatment	$I_A$ [A]	$t_p$ [ $\mu$ s]
1	roughing	80	100
	finishing ( $\times 4$ )	80	100
2	roughing	80	60
	finishing ( $\times 4$ )	80	60
3	roughing	56	60
	finishing ( $\times 4$ )	56	60

4	roughing	56	100
	finishing ( $\times 4$ )	56	100
5	roughing	40	100
	finishing ( $\times 4$ )	40	100
FeAl+ nano-Al <sub>2</sub> O <sub>3</sub>			
Treatment option	Type of treatment	$I_A$ [A]	$t_p$ [ $\mu$ s]
1	roughing	80	100
	finishing ( $\times 4$ )	80	100
2	roughing	56	100
	finishing ( $\times 4$ )	56	100
3	roughing	40	100
	finishing ( $\times 4$ )	40	100

parameters. For undoped FeAl sintered material WEDM trials were carried out by 10 variants (Tab. 2). Based on the analysis of influence of the parameters of applied electroerosion treatment for undoped FeAl sinters, 6 variants of WEDM for materials doped with 2% vol. nano- $\text{Al}_2\text{O}_3$  were selected (Tab. 2).

The surface of the samples directly after WEDM process were observed by PHILIPS XL30/LaB<sub>6</sub> scanning electron microscope equipped with backscattered electron (BSE) detector, which allows to observe differences in the chemical composition (“compo” image), or topography (“topo” image). The state of macro surface texture (ST) of sinters after WEDM treatment was analyzed in macroscopic approach on the basis of research conducted on the contact PGM-1C profilometer. Based on the obtained roughness profile amplitude parameter  $R_a$  was determined. For investigated samples three-dimensional roughness profiles were recorded. In order to quantitatively designate the surface texture parameters (ST), crucial to abrasive wear, the Abbott-Firestone load capacity curves [45-48] were plotted. In the case of forming the surface layer by means of WEDM treatment the obtained curves have a degressive-progressive character. Therefore, the linearization of obtained curves was carried out and the reduced parameters of surface texture (ST) determining theoretical resistance to abrasive wear were designated [48]:

- $Rk$  – kernel or core roughness depth – effective depth of roughness after running,
- $Rpk$  – “reduced” height peak amplitude – surface, which quickly becomes “wiping” after starting work – wear resistance,
- $Rvk$  – “reduced” height valley amplitude – the ability of the surface to maintain lubricant,
- $Mr1$  – threshold as the minimal AHD (asperities height distribution),
- $Mr2$  – threshold as the maximal AHD.

Linearization of load capacity curve was carried out by setting a regression line (linearizing) for the “central region” of the curve, covering 40% of all designated points of the profile (Fig. 3). This area is located in that part of the curve where the plotted secant above 40% of the fraction of material has the smallest angle of inclination of the analyzed curve.

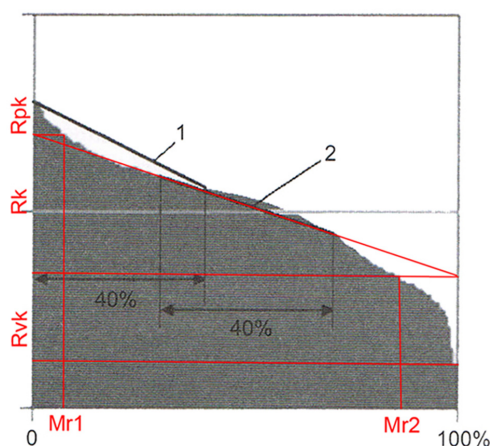


Fig. 3. Determination of the linearizing straight line for the load capacity curve: 1 – secant, 2 – linearization line [47]

## 4. Results and discussion

### 4.1. Surface roughness of FeAl sinters after WEDM process

In Figure 4 the values of the roughness parameter  $R_a$  of both kind of sinters after WEDM treatment were presented. The  $R_a$  parameter – arithmetic mean deviation of the assessed profile – was adopted as a representative parameter of the surface texture (ST).

It has been found (Fig. 4a) that the value of  $R_a$  parameter only slightly depends on the type of machining (roughing or finishing).

The obtained results for FeAl sinters indicates, that reduction of the time of interval between individual impulses causes an increase of  $R_a$  parameter (comparison: variant 1 with 2 and variant 4 with 3). The surface roughness also increases with an increase of current value, with maintaining the constant value of time of interval duration (comparison: variant 1 with 4 and variant 2 with 3). It was observed, that for the smallest value of current (40 A)  $R_a$  parameter is at comparable level, as in the case of cutting with a current intensity equal 56 A. The maximum height of roughness ( $R_a = 2,68 \mu\text{m}$ ) was found for surface after finishing conducted with the highest values of current equal 80 A and the shortest time of interval between impulses ( $t_p = 60 \mu\text{s}$ ). In case of treatment of sinters without ceramic, the smallest value of parameter  $R_a = 1,97 \mu\text{m}$  (variant 4 – finishing) was recorded for finishing with  $t_p = 100 \mu\text{s}$  and  $I_A = 56 \text{ A}$ . The value of  $R_a$  parameter decreased about 14,4% compared to surface obtained in variant 1 – finishing.

In case of materials doped with 2% vol.  $\text{Al}_2\text{O}_3$  nanoceramic, reduction of value of  $R_a$  parameter with decreases of value of current was observed (Fig. 4b). The biggest difference (13,1%) between roughness after finishing and roughing was obtained for option 3 (Fig. 4b). For the surface after finishing, according to option 3 ( $I_A = 40 \text{ A}$ ,  $t_p = 100 \mu\text{s}$ ), the value of parameter  $R_a = 1,46 \mu\text{m}$  was recorded.

Effect of „smoothing” of sinter surface due the addition of nanoceramic, can be explained by the presence of homogeneously distributed, dispersion nano- $\text{Al}_2\text{O}_3$  oxide phase. As a result of roughing electroerosion treatment melting and evaporation of the matrix material (FeAl intermetallic phase) takes place. Since ceramic does not subject to melting and erosion, it creates a thermal barrier, which fills the bottom of the crater. During the finishing, which is carried out without treated surface penetration, protruding peaks of craters are smoothed, and ceramic plays role of dielectric limiting the melting of matrix material. As consequence, there is no formation a new and deepening of already existing craters.

Microscopic analysis (BSE detector – “topo” view mode) of the surface of sinters with and without nanoceramic after finishing demonstrated, that the surface has an isotropic character independently on applied treatment parameters (Fig. 5). The size of craters on investigated surfaces mainly depends on

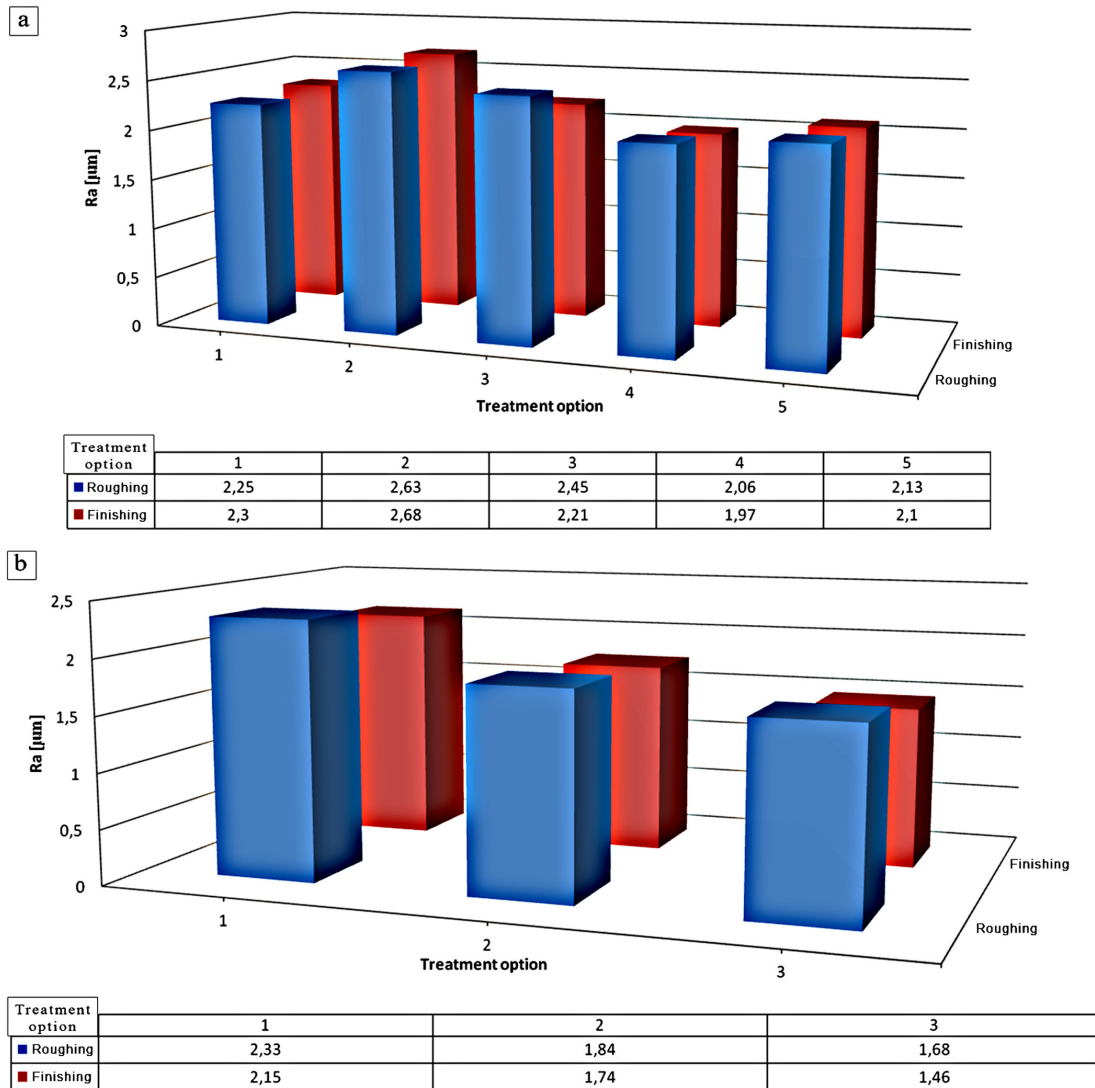


**Fig. 4.** Roughness parameter ( $R_a$ ) of sinters surface after wire electric discharge machining (WEDM): a) sinters FeAl, b) sinters FeAl+nano- $\text{Al}_2\text{O}_3$

values of impulse energy ( $e_i$ ). In simple way, the impulse energy is calculated from the formula:

$$e_i = U_{Ar} * I_{Ar} * t_i \text{ [J]} \quad (1.1)$$

where:  $U_{Ar}$  – the amplitude of operating voltage [V],  $I_{Ar}$  – the amplitude of current working [A],  $t_i$  – impulse time [s].

Depending on the impulse energy, a different deep and a diameter of single cavity are obtained – the smaller is value of impulse energy, that these values are also smaller. For the accepted dependence the impulse energy has the following values of the current:

$$I_A = 40 \text{ A} - 0,037 \text{ J},$$

$$I_A = 56 \text{ A} - 0,052 \text{ J},$$

$$I_A = 80 \text{ A} - 0,074 \text{ J}.$$

The obtained results of measurements of roughness parameters of surface confirm theoretical positive dependence of surface roughness from impulse energy.

The macroscopic evaluation of the surface layer of sinters indicates on isotropic character of surface after WEDM treatment

also in macro scale. The obtained spatial, unfiltered roughness profiles of surface for each option of treatment (Fig. 6) are comparable with the micro images of surface (Fig. 5). In case of FeAl sinter surface, the analysis of surface roughness (unfiltered profile) after final cut confirms, that reduction of interval time ( $t_p = 60 \mu\text{s}$ ) adversely affects the quality of obtained surface – increase of roughness to  $P_c = 8,12 \mu\text{m}$  (Fig. 6b) was observed. However, application a longer interval time and smaller value of current intensity leads to smoothing of sinter surface, as evidenced by obtained  $5,03 \mu\text{m}$  height of roughness (Fig. 6a).

It was found, independently on accepted parameters of electroerosion treatment, that for the sinters with addition of nanoceramic the quality of surface after cutting (Fig. 6c) is higher than for material without nano –  $\text{Al}_2\text{O}_3$  (Fig. 6a and 6b). In case of cutting sinter without ceramic, reduction of current intensity to 40 A and increase of the interval time to  $100 \mu\text{s}$ , leads to „surface smoothing“ to the level of  $P_c = 4,02 \mu\text{m}$  (Fig. 6c).

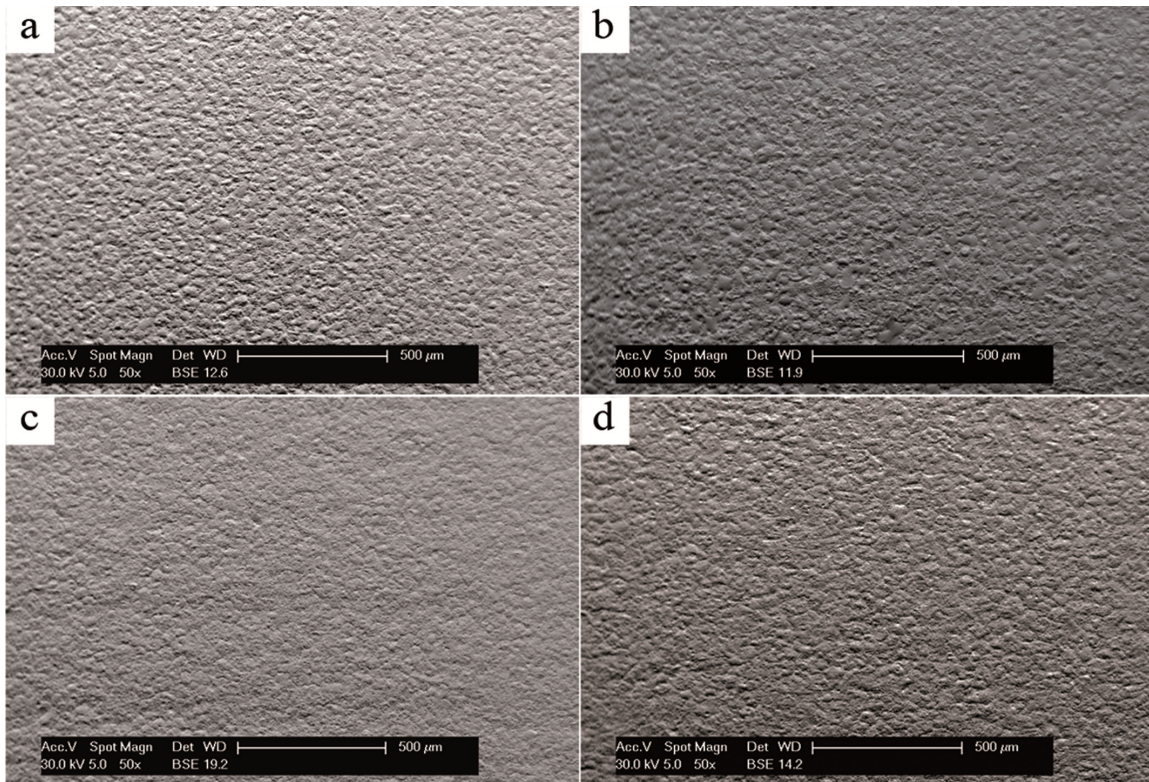


Fig. 5. Surface topography of sinters after finishing WEDM: a) FeAl ( $I = 56$  A,  $t_p = 100$   $\mu$ s), b) FeAl ( $I = 80$  A,  $t_p = 60$   $\mu$ s), c) FeAl+2% vol. nano- $\text{Al}_2\text{O}_3$  ( $I = 40$  A,  $t_p = 100$   $\mu$ s), d) FeAl+2% vol. nano- $\text{Al}_2\text{O}_3$  ( $I = 80$  A,  $t_p = 100$   $\mu$ s)

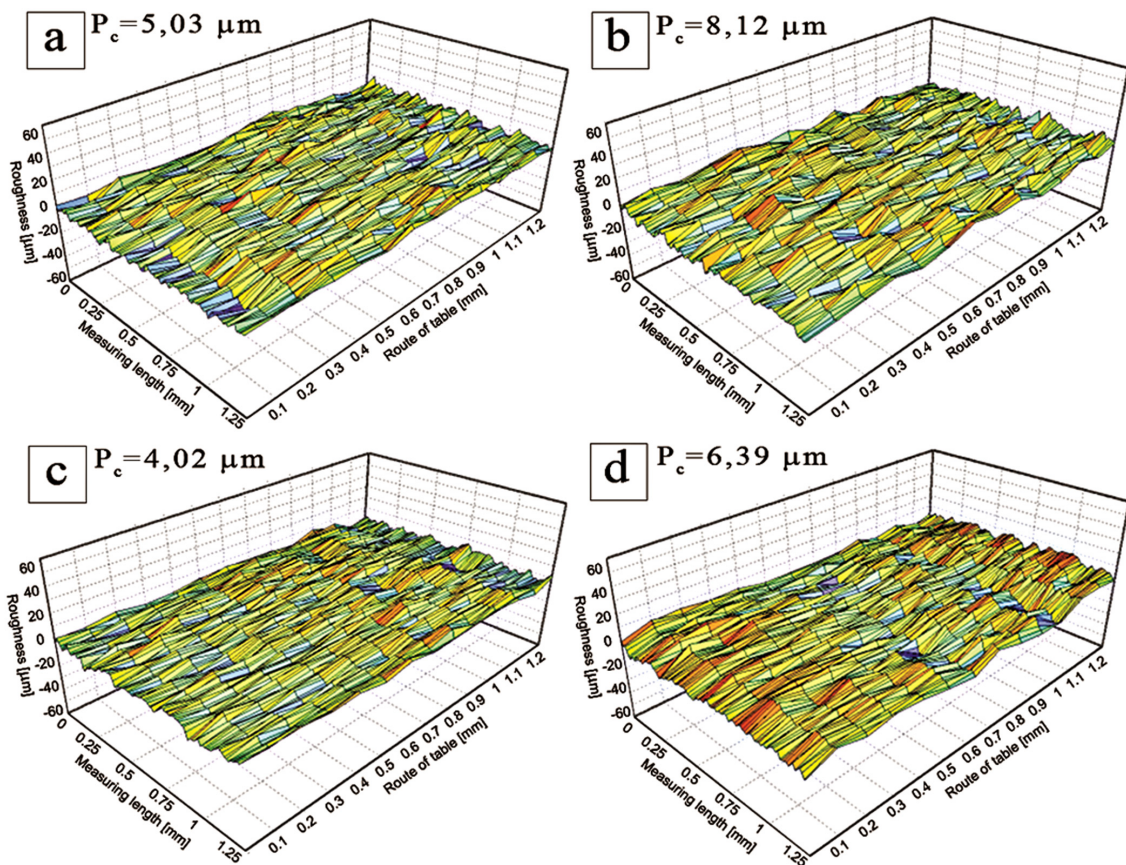


Fig. 6. 3D profiles of sinter surface after finishing WEDM: a) FeAl ( $I = 56$  A,  $t_p = 100$   $\mu$ s), b) FeAl ( $I = 80$  A,  $t_p = 60$   $\mu$ s), c) FeAl+2% vol. nano- $\text{Al}_2\text{O}_3$  ( $I = 40$  A,  $t_p = 100$   $\mu$ s), d) FeAl+2% vol. nano- $\text{Al}_2\text{O}_3$  ( $I = 80$  A,  $t_p = 100$   $\mu$ s)

### 4.2. Analysis of capacity load curves of FeAl sinters after WEDM

The analysis of load capacity of the sinters surface after WEDM was realized for three technological variants for both kind of sinters. The first variant included roughing and finishing treatment with initial parameters, while the second and the third options were treatments with parameters for which the biggest and smallest surface roughness were obtained, respectively.

Figure 7 shows typical load capacity curves for chosen contour lines of the 3D profile. The analyzed curves have degressive – progressive character (with inverted s-letter like shape), which is typical for surface with randomly distributed roughness. On

the basis of the Abbott-Firestone curves following parameters were estimated: the reduced height of peaks *Rpk* and depth of the cavities *Rvk*, core roughness height *Rk* and fraction of load capacity peaks *Mr1* and cavities *Mr2*. Significant difference between the *Mr1* and *Mr2* parameters and the low value of the *Rk* allows concluding about high load capacity of the sinters surface (Fig. 7).

Values of reduced parameters of load capacity characterizing the surface of investigated sinters are different, depending on accepted technological variants of used EDM treatment (Tab. 3). The reduced parameters of load capacity change significantly versus accepted tribological parameters, both for sinters with and without nanoceramic  $Al_2O_3$ .

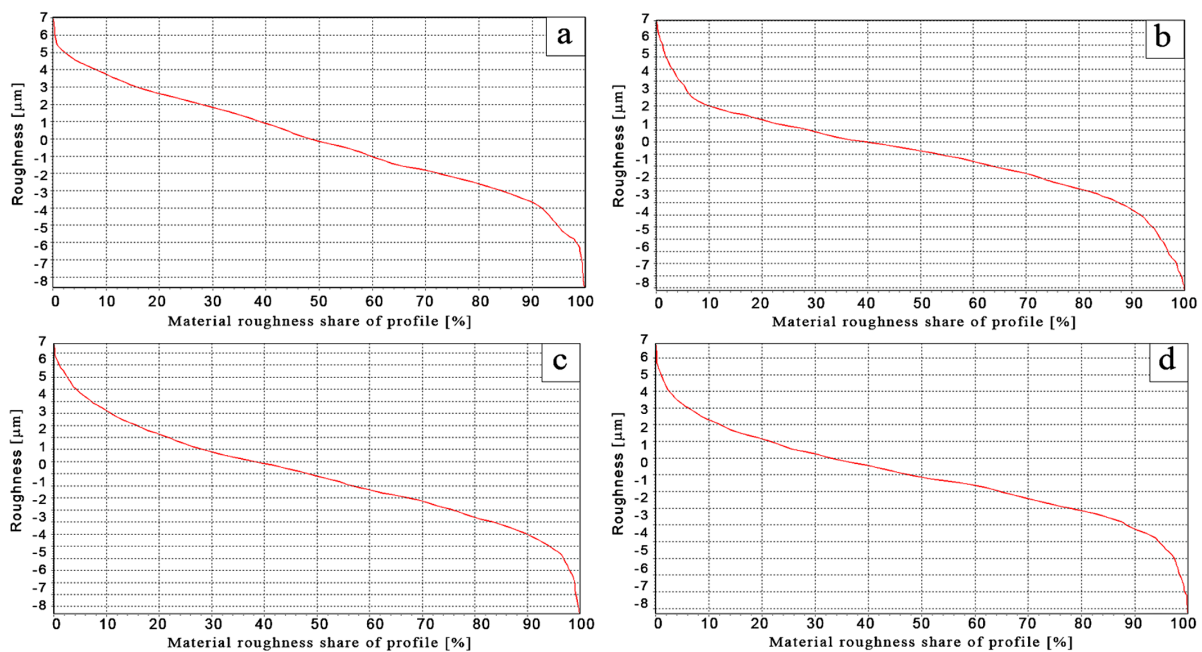


Fig. 7. Load capacity curve of sinters after finishing WEDM: a) FeAl ( $I = 56\text{ A}$ ,  $t_p = 100\ \mu\text{s}$ ), b) FeAl ( $I = 80\text{ A}$ ,  $t_p = 60\ \mu\text{s}$ ), c) FeAl+2% vol. nano –  $Al_2O_3$  ( $I = 40\text{ A}$ ,  $t_p = 100\ \mu\text{s}$ ), d) FeAl+2% vol. nano –  $Al_2O_3$  ( $I = 80\text{ A}$ ,  $t_p = 100\ \mu\text{s}$ )

TABLE 3

Parameters of load capacity curve for FeAl and FeAl+nano- $Al_2O_3$  sinters surface after WEDM process. Treatment variants: 1 – with initial parameters, 2 – for the biggest roughness after WEDM, 3 – for the smallest roughness after WEDM

Material/Parameters of treatment	Parameters of load capacity curves					
	<i>Rpk</i> [µm]	<i>Rvk</i> [µm]	<i>Rk</i> [µm]	<i>Mr1</i> [%]	<i>Mr2</i> [%]	<i>Mr2-Mr1</i>
<b>FeAl sinter</b>						
1 – roughing $[I_A = 80\text{ A}; t_p = 100\ \mu\text{s}]$	3,6	2,9	7,4	9	89	80
1 – finishing $[I_A = 80\text{ A}; t_p = 100\ \mu\text{s}]$	3,2	4,8	8,5	5	92	87
2 – roughing $[I_A = 80\text{ A}; t_p = 60\ \mu\text{s}]$	6,6	2,5	9,6	6	95	89
2 – finishing $[I_A = 80\text{ A}; t_p = 60\ \mu\text{s}]$	6,4	7	8,8	7	88	81
3 – roughing $[I_A = 56\text{ A}; t_p = 100\ \mu\text{s}]$	3	3	8,2	5	94	89
3 – finishing $[I_A = 56\text{ A}; t_p = 100\ \mu\text{s}]$	2,4	3,8	9,2	5	94	89

FeAl + 2% vol. nano- $Al_2O_3$ sinter	<i>Rpk</i> [µm]	<i>Rvk</i> [µm]	<i>Rk</i> [µm]	<i>Mr1</i> [%]	<i>Mr2</i> [%]	<i>Mr2-Mr1</i>
1 – roughing $[I_A = 80\text{ A}; t_p = 100\ \mu\text{s}]$	6,8	4,5	7,6	9	90	81
1 – finishing $[I_A = 80\text{ A}; t_p = 100\ \mu\text{s}]$	4,7	4,8	6,7	10,5	92	81,5
2 – roughing $[I_A = 56\text{ A}; t_p = 100\ \mu\text{s}]$	5,2	7,7	5,7	9,5	88,5	79
2 – finishing $[I_A = 56\text{ A}; t_p = 100\ \mu\text{s}]$	3,6	9,1	5,2	10	90	80
3 – roughing $[I_A = 40\text{ A}; t_p = 100\ \mu\text{s}]$	2,6	3,2	6	9	90	81
3 – finishing $[I_A = 40\text{ A}; t_p = 100\ \mu\text{s}]$	2,4	3,8	5,6	9	93	84

The reduced height of  $R_{pk}$  peaks determines this part of the surface, which will be removed during lapping, in an early stage of work. This parameter may be considered as a metric of wear resistance of investigated surface.

For sinter without addition of ceramic there was no effect of the type of used treatment (finishing, roughing) on the value of  $R_{pk}$  parameter, what indicates on the absence of necessity for using the finishing. In the case of nano- $Al_2O_3$  doped material, it was observed, that finishing improves the theoretical wear resistance of the surface, excluding the variant conducted with current intensity  $I_A = 40$  A and interval time  $t_p = 100 \mu s$ , for which  $R_{pk}$  parameter is on the same level, independently on the applied treatment. One should notice, that current intensity has significant impact on  $R_{pk}$  – reduction of its value lead to decrease of  $R_{pk}$  parameter.

The smallest value of  $R_{pk}$  parameter (and thus the highest theoretical abrasive wear resistance), equal to  $2.4 \mu m$  was found for the surface after finishing treatment with a current intensity  $I_A = 56$  A and an interval time  $t_p = 100 \mu s$  for sinters without addition of nanoceramic. While for sinter doped with nano- $Al_2O_3$  the best result was obtained for finishing with interval time  $t_p = 100 \mu s$  and current intensity equal to 40 A.

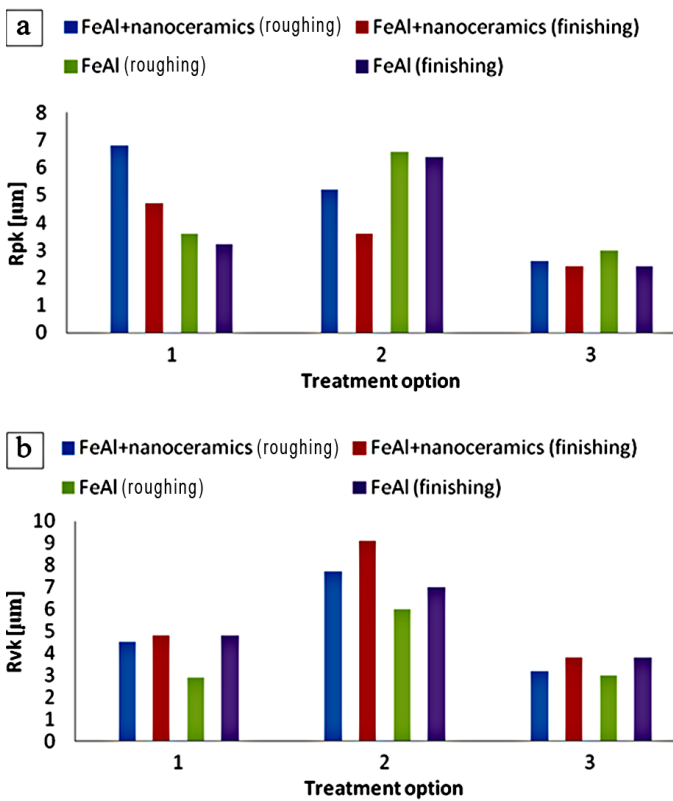


Fig. 8. Influence of WEDM parameters on the  $R_{pk}$  (a) and  $R_{vk}$  (b) values for sinters with and without nano- $Al_2O_3$

Analyzing the influence of treatment parameters on value of  $R_{vk}$  parameter (the ability of the surface to maintain lubricant) (Fig. 8b) it was found, that for sinters without addition of ceramic reduction of interval time ( $t_p = 60 \mu s$ ) leads to increase of  $R_{vk}$

parameter (roughing and finishing). On the other hand, reduction of current intensity ( $I_A = 56$  A) does not cause any changes after roughing, except only a small decrease of  $R_{vk}$  value after finishing. Also it was observed, that execution of finishing treatment (independently of value of its technological parameters) causes increase of obtained deep of cavities after roughing.

Increase of  $R_{vk}$  parameter after finishing with current  $I_A = 56$  A and interval time  $t_p = 100 \mu s$  for sinter doped with  $Al_2O_3$  nanoceramic was found. After roughing with the same values of parameters, the influence of type of treatment (roughing, finishing) was not noted. In case of treatment with current  $I_A = 40$  the surface has a low value of  $R_{vk}$  parameter equal to  $3.2 \mu m$ . The highest ability to maintain the lubricant was shown by the sintered material doped with  $Al_2O_3$  nanoceramic, after finishing with current  $I_A = 56$  A and interval time  $t_p = 100 \mu s$ .

The value of height of core roughness is independent on reduced depth of peaks and valleys of profile. Based on the analysis of influence of treatment parameters on  $R_k$  it was found, that the highest capacity after lapping had the sinter after finishing carried out according to variant 2 ( $I_A = 56$  A,  $t_p = 100 \mu s$ ) –  $R_k = 5.2 \mu m$ .

For material without addition of nano- $Al_2O_3$  the value of parameter  $R_k$  is constant for all treatment options. Simultaneously, for sinter with addition of nanoceramic a decrease of core roughness after reduction of current to 56 A and keeping the value of  $R_k$  parameter on similar level than for treatment with current 40 A, was observed. Also it was found, that the type of treatment (finishing, roughing) has no effect on the value of surface roughness after time of lapping for sinter doped with nano- $Al_2O_3$ .

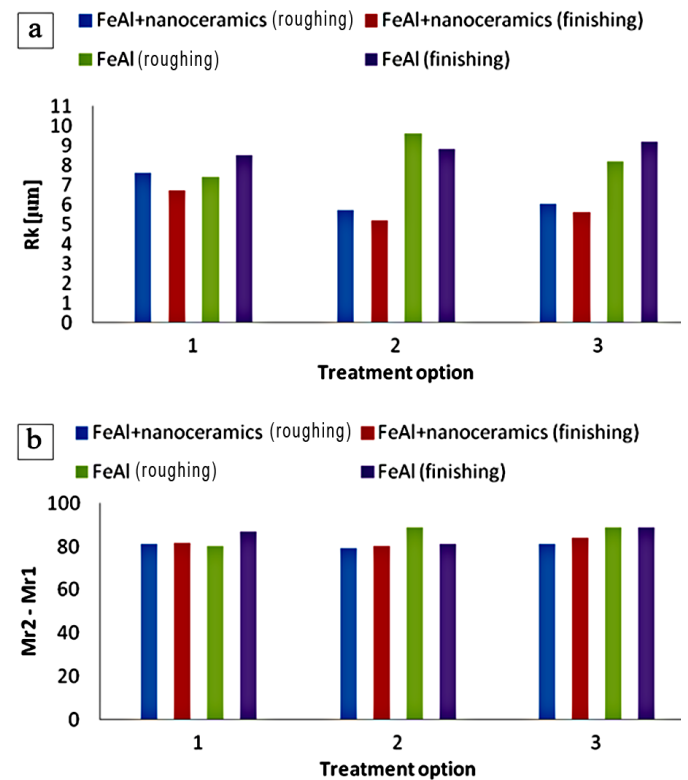


Fig. 9. Influence of WEDM parameters on the value of  $R_k$  parameter (a) and the difference between the parameter  $Mr_2$  and  $Mr_1$  (b) for sinters with and without nano- $Al_2O_3$



A large difference between the bearing fractions of the vertices  $Mr1$  and cavities  $Mr2$  for surface of sinters without and with nanoceramic is comparable for all considered cases and gives a proof of high capacity of surface of sinters.

## 5. Conclusions

Based on analysis of obtained results it was found, that there is a possibility of introducing electroerosion treatment to FeAl based sintered materials with and without addition of oxide nanoceramics  $Al_2O_3$ . Parameters and type of EDM treatment (roughing, finishing) can substantially affect surface texture (ST), and thus wear resistance or ability to maintenance the lubricant. Sintors doped by  $Al_2O_3$  nanoceramic have much lower surface roughness after electroerosion treatment compared to sinters without addition of nano- $Al_2O_3$ . Analysis of sinters surface without addition of ceramic, after multivariate electroerosion cutting, demonstrates that the smallest roughness ( $R_a = 1,97 \mu m$ ) was obtained for surface after finishing (four sparking passes) with current intensity  $I_A = 56 A$  and interval time  $t_p = 100 \mu s$ . The highest theoretical smoothing of sinters surface with addition of 2% vol. nano- $Al_2O_3$  was obtained after finishing with following parameters:  $I_A = 40 A$  and  $t_p = 100 \mu s$ . The highest abrasive wear resistance ( $R_{pk} = 2,4 \mu m$  – the same for both material) was noted for sinters surface without addition of ceramic after finishing with interval time  $t_p = 100 \mu s$  and current intensity  $I_A = 56 A$ . For surface of sinter doped with nanoceramic similar effects were obtained after finishing with interval time  $t_p = 100 \mu s$  and current intensity  $I_A = 40 A$ . It was found, that material with addition of nano- $Al_2O_3$  after finishing with parameters equal to  $t_p = 100 \mu s$  and  $I_A = 56 A$ , exhibit the highest load capacity of surface after lapping time ( $R_k = 5,2 \mu m$ ), as well as the largest ability to maintain lubricant ( $R_{vk} = 9,1 \mu m$ ).

## REFERENCES

- [1] T. Durejko, Z. Zarański, S. Sulej, *Kompozyty (Composites)* **8**, 2, 190-194 (2008).
- [2] A.K. Khanra, S. Patra, M.M. Godkhindi, *Bull. Mater. Sci.* **29**, 3 (2006).
- [3] M. Trzaska, J. Perończyk, D. Biało, *Kompozyty*, 4, (2004).
- [4] N.M. Abbas, D.G. Solomon, Md. Fuad Bahari, *Int. Journal of Machine Tools & Manufacture* **47**, (2005).
- [5] J. Perończyk, D. Biało, *Kompozyty*, 1, (2001).
- [6] M. Trzaska, J. Perończyk, D. Biało, *Kompozyty*, 5, (2005).
- [7] T. Durejko, M. Ziętała, M. Łazińska, *Kompozyty (Composites)* **11(3)**, 258-263 (2011).
- [8] K. Kowalski, B. Łosiewicz, A. Budniok, M. Kupka, *Materials Chemistry and Physics* **126**, 314-318 (2011).
- [9] D.G. Moris, *Intermetallics* **6**, 753-758 (1998).
- [10] R.S. Sundar, S.C. Deevi, *Material Science and Engineering* **357**, 124-133 (2003).
- [11] S.C. Deevi., *Materials Science and Engineering* **573**, A329-331 (2002).
- [12] W. Szkliniarz, A. Kościelna, *Inżynieria materiałowa*, 2, 72-76 (2008).
- [13] W. Szkliniarz, E. Mikuszewski, *Inżynieria materiałowa* **155**, 4-5 (2003).
- [14] I. Bednarczyk, D. Kuc, G. Niewielski, *Archives of Metallurgy and Materials* (2014), DOI: 10.2478/amm-2014-0191
- [15] C. Senderowski, *J. Thermal Spray Technol.* **23(7)**, 1124-1134 (2014).
- [16] W. Wołczyński, C. Senderowski, J. Morgiel, G. Garzeł, *Archives of Metallurgy and Materials* **59(1)**, 211-220 (2014).
- [17] A. Pawłowski, C. Senderowski, Z. Bojar, M. Faryna, *Archives of Metallurgy and Materials* **55(4)**, 1061-1071 (2010).
- [18] A. Pawłowski, C. Senderowski, W. Wołczyński, J. Morgiel, Ł. Major, *Archives of Metallurgy and Materials* **56(1)**, 71-79 (2011).
- [19] A. Pawłowski, T. Czepe, Ł. Major, C. Senderowski, *Archives of Metallurgy and Materials* **54(3)**, 783-788 (2009).
- [20] C. Senderowski, Z. Bojar, W. Wołczyński, G. Roy, T. Czujko, *Archives of Metallurgy and Materials* **52(4)**, 569-578 (2007).
- [21] C. Senderowski, A. Pawłowski, Z. Bojar, W. Wołczyński, M. Faryna, J. Morgiel, Ł. Major, *Archives of Metallurgy and Materials* **55(2)**, 373-381 (2010).
- [22] A. Pawłowski, C. Senderowski, Z. Bojar, J. Bonarski, Ł. Major, *Archives of Metallurgy and Materials* **56(2)**, 263-269 (2011).
- [23] C. Senderowski, D. Zasada, T. Durejko, Z. Bojar, *Powder Technology* **263**, 96-103 (2014).
- [24] C. Senderowski, M. Chodała, Z. Bojar, *Materials* **8(3)**, 1108-1123 (2015).
- [25] Y Chen, H.M. Wang, *Surf. Coat. Technol.* **168**, 30-36 (2003).
- [26] B. Benjamin, M. Schäfer, C. Pauly, F. Mücklich, *Surf. Coat. Technol.* **235**, 773-777 (2013).
- [27] S.F. Corbin, E. Toyserkani, A. Khajepour, *Mat. Sci. and Eng.* **354**, 48-57 (2003).
- [28] B. Abdolahi, H.R. Shahverdi, M.J. Torkamany, M. Emami, *Appl. Surf. Sci.* **257**, 9921-9924 (2011).
- [29] T. Durejko, P. Józwick, Z. Bojar, *Archives of Metallurgy and Materials* **54(4)**, 717-723, (2009).
- [30] T. Durejko, S. Lipiński, Z. Bojar, J. Bystrzycki, *Materials & Design* **32**, 2827-2834, (2011).
- [31] M. Łazińska, T. Durejko, S. Lipiński, W. Polkowski, T. Czujko, R.A. Varin, *Materials Science and Engineering, A* **06**, 407-414, (2015).
- [32] T. Durejko, M. Ziętała, Z. Bojar, *Materials* **8(2)**, 575-585, (2015).
- [33] T. Durejko, M. Ziętała, W. Polkowski, T. Czujko, *Materials and Design* **63**, 766-774, (2014).
- [34] C. Garcia Oca, M.A. Munoz-Morris, D.G. Morris, *Intermetallic* **11**, 425-434 (2003).
- [35] D.G. Morris, I. Gutierrez-Urrutia, M.A. Munoz-Morris, *International Journal of Plasticity* **24** (2008).
- [36] K. Wolski, F. Thevenot, J. Le Coze, *Scripta Materialia* **34**, 5 (1996).
- [37] Z. Bojar, W. Przetakiewicz, *Metallic materials with intermetallic phases*, Warszawa 2006.
- [38] A. Patejuk, T. Durejko, *Przegląd Mechaniczny*, 3 (2005).

- [39] F. Weng, M. Her, Int. J. Adv. Manuf. Technol. **19**, 266-270 (2002).
- [40] S. Yeo, G. Yap, Int. J. Adv. Manuf. Technol. **18**, (2001).
- [41] J. Qu, A. Shih, R. Scattergood, ASME **124**, 702-707 (2002).
- [42] A. Muttamara, Y. Fukuzawa, N. Mohri, T. Tani, J. Mater. Process. Technol. **140**, 243-247 (2003).
- [43] N. Mohri, Y. Fukuzawa, T. Tani, Ann. CIRP **51**, 112-116 (2002).
- [44] T. Durejko, A. Strak, S. Lipiński, Kompozyty (Composites) **11** (3), 225-229 (2011).
- [45] J. Tomasik, D. Biało, Mechanik **1**, 26-28 (2003).
- [46] K.E. Oczos, V. Liubimov, Surface geometry, Rzeszów 2003.
- [47] S. Adamczak, Surface geometry metrology. Outlines of shape, waviness and roughness, Warszawa 2008.
- [48] M. Bigerelle, A. Iost, Tribology International **40**, 1319-1334 (2007).

*Received: 20 April 2015.*